Laboratory Investigation of Halite Precipitation in Large Scale Bead Packs

Introduction

When CO_2 is injected into the subsurface, such as saline aquifers, for long term storage there is a risk of salt precipitation near the wellbore. As the dry gas flows into the porous rock it both displaces and evaporates the resident water. With sufficient evaporation, the resident brine will become supersaturated (usually with NaCl) and salt will precipitate (Halite). Continued precipitation will result in blockage of the pores, reduction in permeability, and eventually, full occlusion of the porous medium. It is worth noting that due to corrosion risks – where even a small volume of water in the CO_2 stream can cause severe degradation of the tubing integrity – the gas must be injected dry (Cole *et al.* 2011).

Previous studies have typically focused on numerical simulation (Ogundipe and Mackay 2025; Zamani *et al.* 2026), micromodels (Miri *et al.* 2015), or corefloods (Sokama-Neuyam *et al.* 2019). However, here we present large, Darcy-scale glass bead packs which represent both the porous medium and the well. This allows for direct visualization of the fluid displacement in the porous medium (viscous fingering/capillary fingering/gravity segregation) and of the salt formation at the injection face (as observed at the Aquistore project (Talman *et al.* 2020)). Representing the subsurface in this manner allows for direct scaling to an equivalent field system (Gaucher and Lindley 1960; Sorbie 2025). One of the key literature observations relevant to the results presented here is related to the properties of the halite itself. Miri *et al.* (2015) observed that the halite crystals acted as a highly hydrophilic porous medium which could strongly imbibe the saline brine. This resulted in a self-enhancing mechanism where further salt growth resulted in a higher surface area for evaporation, in turn causing more salt to precipitate, and in turn further imbibe brine.

Here we use dry N_2 as an analogue to CO_2, which simplifies the experimental process. As the experiments are carried out at ambient conditions, the flow properties of the two gases are relatively similar. Indeed, their evaporative properties are also very similar – especially around ambient conditions – see *Figure 1*, where a series of thermodynamic calculations were performed using OLI ScaleChem to compare the moles of water evaporated by a stream of 100 moles of CO_2 vs N_2 at a range of pressures and temperatures.

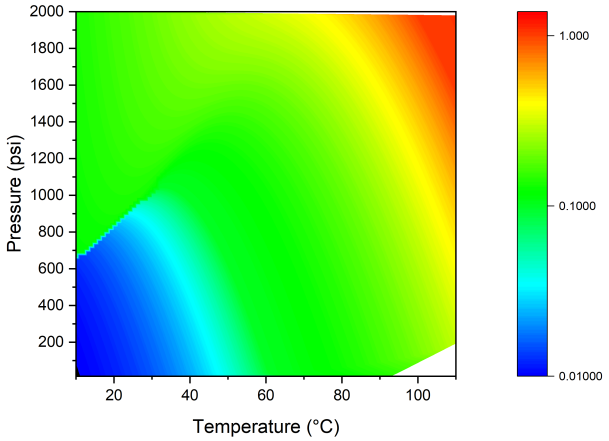

Figure 1 Difference in the number of moles of water evaporated into a stream of 100 moles of CO_2 vs the number of moles of water evaporated into a stream of 100 moles N_2 at a range of pressures and temperatures. Note the discontinuity on the transition from gaseous CO_2 to liquid CO_2 ~700 psi.

Methodology

The visualized experiment was conducted in a large glass bead pack. The porous medium consisted of glass ballotini beads (125-350 µm) which were slurry packed into a Perspex cell of dimensions 18x14x1.5 cm. Fluid injection was performed along the short edge of the pack as shown in *Figure 2*.

The inlet port consists of a large open channel, separated from the porous medium by a perforated plastic sheet and a fine mesh to prevent ingress of the glass beads.

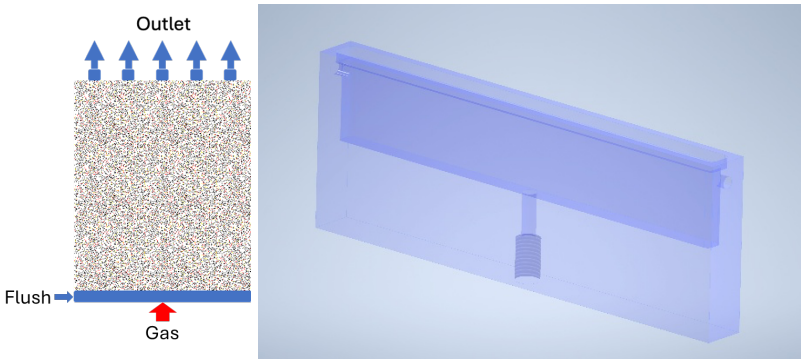

Figure 2 Schematic of the bead pack design (left) and a render of the injection port (right).

This design of inlet channel allows for flushing of the injection port prior to fluid injection and direct visualization of the "well" of the beadpack. Fluids are produced through 5 equally spaced ports at the opposite end of the pack, which co-mingle into a single effluent line. The pack properties are given in *Table 1*.

Table 1 Glass bead pack properties.

Property	Value
Dimensions (cm)	18x14x1.5
Porosity, *f*	0.33
Pore Volume (ml)	125
Permeability (D)	9.5

The resident brine is 200 g/L NaCl dyed blue with 0.25 g/L Erioglaucine. Oxygen free nitrogen is injected using an Alicat MC mass flow controller set to 45 cc/min, supplied at 1 bar. This is equivalent to an advancement rate of 308 ft/day. Injection is performed bottom-to-top where gravity forces act in the direction of flow.

Results

Figure 3 shows the displacement pattern in the porous medium for the bottom-to-top displacement, where dry N_2 is continually injected for >5,000 PV.

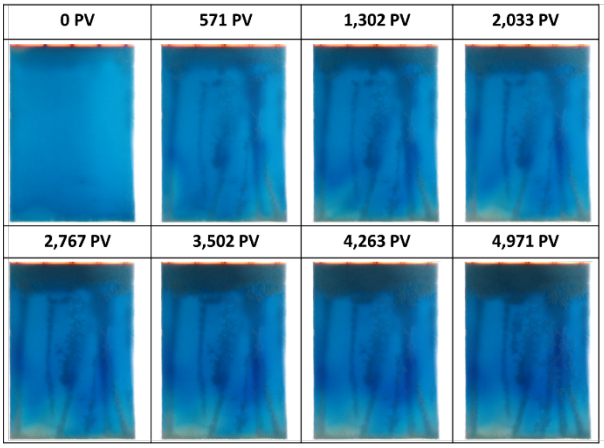

Figure 3 Stepwise progression of fluid distribution during bottom-to-top injection of gas to displace the resident blue brine (200 g/L NaCl). Injection volume given in terms of pore volumes injected (PV).

As the injection period is so long, only the long term behavior is emphasized here; the gas fingered readily through the porous medium giving a very inefficient displacement. Following this, there was little further finger development (as expected). When further fingers were developed, this is likely due to blockage of the fluid inlet in a specific location, rediverting fluid flow. The main change to the fluid distribution in the porous medium is the growth of the high gas saturation area at the top of the pack. We interpret this as gravity/capillary forces driving the water to the dry zone at the bottom of the pack countercurrently, rather than a build-up of injected gas at the pack exit. A close view of the injection channel ("well") is given in *Figure 4* for the same time intervals.

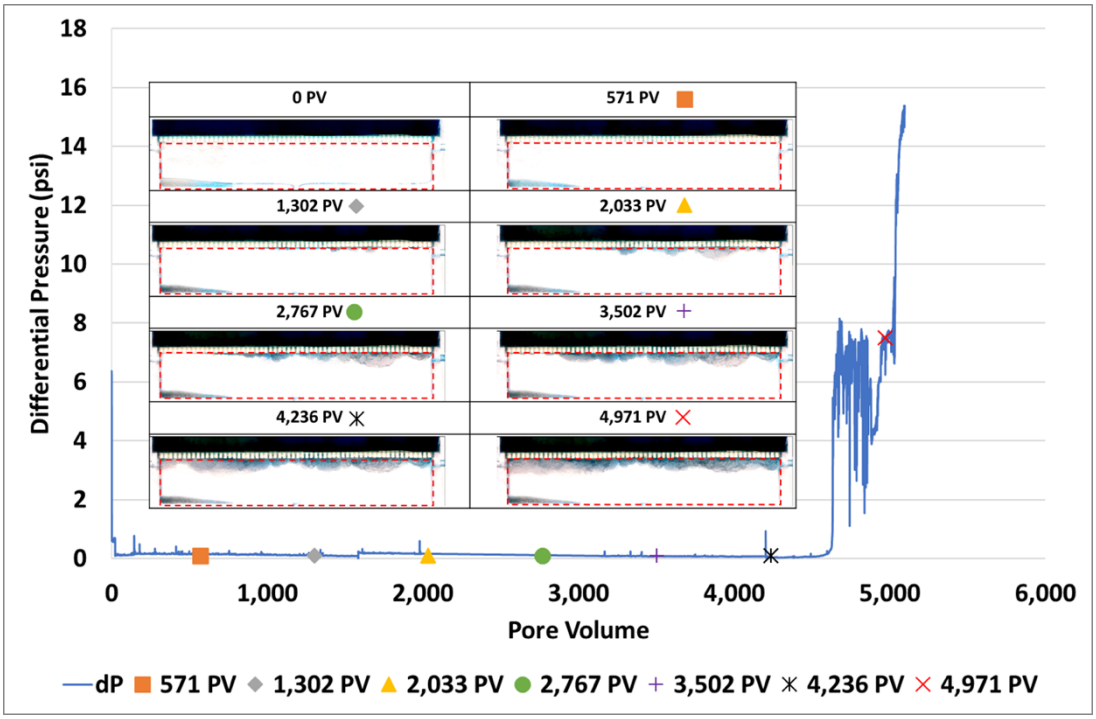

Figure 4 Stepwise progression of salt build-up during bottom-to-top injection of gas to displace the resident brine (200 g/L NaCl) overlaid on a plot of differential pressure across the pack. The symbols indicate the point on the differential pressure plot where the image was obtained.

Salt formation can be observed between 517 and 1,302 PV (~26-60 hours of injection), initially localized around the right hand side of the pack where the largest number of fingers are formed. As injection continues the halite continues to grow – initially on the walls of the channel, spreading out across the whole injection length, before finally the salt bridges across the perforations and blocks the injection face. This causes the initial pressure increase at ~4,600 PV, where the pressure differential increases but the injection rate remains constant before a secondary increase ~5,100 PV which reduces the permissible flow rate to zero. Note that as the mass flow controller is supplied at ~1 bar, it is only able to provide stable flow up to that pressure.

Conclusions

Gas breakthrough was rapid and was highly inefficient, dominated by a small number of fine fingers leaving the majority of the resident brine in place. As gas injection continued there was little further development of these fingers. From observation of the inlet channel, it is clear that salt formation was primarily in the injection manifold rather than in the porous medium itself. Once salt began to form after ~500 PV of gas injection, the salt began to grow from the injection face along the sides of the channel, eventually spreading to cover the length of the injection area. Despite the high level of salt precipitation observed, injectivity was not impaired until ~4,630 PV where the injection pressure rapidly increased to an interim plateau. After a further 400 PV, the pressure rose to the maximum permissible value and injection rate fell to near zero. Thus, we conclude that while salt formation was evident after

~10% of the total gas had been injected, the deposition occurred in the "well" rather than across the perforations between the "well" and the porous medium – which would block flow. Secondly, we see that the halite preferentially deposits in the driest zone, i.e. the point of injection, and imbibes the saline water from the porous medium into the salt aggregate structure. In line with the observations made by Miri *et al.* (2015) in their micromodel experiments, we find that the growing halite aggregate itself causes significant imbibition of brine from the porous medium and that the salt deposition is self-enhancing. As the halite precipitates it imbibes brine from the porous medium which then evaporates, depositing more salt, and further imbibes brine from the main porous medium.

Future work should consider the observations presented here when assessing the risk of halite formation; specifically, the risk of salt formation on the injection face, as observed in the Aquistore CCS project (Talman *et al.* 2020), rather than deeper in the reservoir as often observed with numerical simulations and micromodels. Secondly, appropriate scaling between laboratory and the field should be considered – ensuring that the balance of forces (viscous, capillary, and gravity) is representative of the field system at the laboratory scale (Sorbie 2025).

Further details of this study have been submitted for publication, along with a second experiment conducted in a "side-to-side" aspect (representing a 2D cross section of a vertical well) where the imbibed brine was observed to cause dissolution/re-precipitation of the growing salt aggregate.

Acknowledgements

The sponsors of the FAST9 joint industry project at Heriot-Watt University (Baker Hughes, Chevron, Clariant, Equinor, Harbour Energy, SLB and Total Energies) are thanked for funding this work. Energi Simulation is thanked for funding the Chair in CCUS and Reactive Flow Simulation held by Eric Mackay. OLI is thanked for provision of the ScaleChem license and Dr Guilia Ness for her assistance with the evaporation calculations.

References

Cole, I.S., Corrigan, P., Sim, S., Birbilis, N.: Corrosion of pipelines used for CO2 transport in CCS: Is it a real problem? *International Journal of Greenhouse Gas Control* **5**(4), 749-756 (2011). https://doi.org/https://doi.org/10.1016/j.ijggc.2011.05.010
Gaucher, D.H., Lindley, D.C.: Waterflood Performance in a Stratified, Five-Spot Reservoir - A Scaled-Model Study. *Transactions of the AIME* **219**(01), 208–215 (1960). SPE-1311. https://doi.org/10.2118/1311-G
Miri, R., van Noort, R., Aagaard, P., Hellevang, H.: New insights on the physics of salt precipitation during injection of CO2 into saline aquifers. *International Journal of Greenhouse Gas Control* **43**, 10-21 (2015). https://doi.org/https://doi.org/10.1016/j.ijggc.2015.10.004
Ogundipe, O.M., Mackay, E.J.: Modelling the Impact of Injection Rate and Heterogeneity on the Extent and Location of Halite Precipitation During CO2 Storage in Saline Aquifers: A Field Case Example. Presented at the SPE Energy Transition Symposium, Sugar Land, Texas, USA, 8-10 September, 2025. SPE-228366. https://doi.org/10.2118/228366-ms
Sokama-Neuyam, Y.A., Ursin, J.R., Boakye, P.: Experimental Investigation of the Mechanisms of Salt Precipitation during CO2 Injection in Sandstone. *C — Journal of Carbon Research* **5**(1), 4 (2019).
Sorbie, K.: Rapoport Revisited: A Review of Scaling Theory of Two Phase Flow in Porous Media and its Application. In: Xu, H., Pan, R., Ke, H., Yang, L. (eds.) Porous Media - Recent Theoretical Approaches and Future Opportunities. IntechOpen, Rijeka (2025)
Talman, S., Shokri, A.R., Chalaturnyk, R., Nickel, E.: Salt Precipitation at an Active CO2 Injection Site. In: Gas Injection into Geological Formations and Related Topics. pp. 183-199. (2020)
Zamani, N., Marban, D.L., Sandve, T.H., Gasda, S.E.: Unraveling salt precipitation mechanisms in geological CO2 storage: insights into dominant driving forces. *InterPore Journal* (2026). https://doi.org/10.69631/zhna7r09